Published online 2023 November 20 **Original Article**

Identification of Biomarkers Associated with Melanoma based on Bioinformatics Analysis

Xuelian Zou[1], Tingting Li[2], Xiangyue Zhang[2] and Xiaojing Kang[1*]

[1] Xinjiang Clinical College, Anhui Medical University, Xinjiang 830001, China
[2] Department of Dermatology and Venereology, People's Hospital of Xinjiang Uyghur Autonomous Region, Xinjiang 830001, China

*** *Corresponding author:*** Xiaojing Kang, Xinjiang Clinical College, Anhui Medical University, 91 Tianchi Road, Urumqi, Xinjiang Uygur Autonomous Region 830001, China. Email: kxiaojing@126.com

Received 2023 April 18 ; **Revised** 2023 May 13 ; **Accepted** 2023 November 10 .

Abstract

Background: Melanoma is an aggressive tumor caused by melanocytes characterized by a poor prognosis at the stage of metastasis. Therefore, it is crucial to identify biomarkers for progression and prognosis for the treatment of melanoma.
Objectives: The study aimed to identify the specific genes related to the prognosis of melanoma utilizing bioinformatics analyses.
Methods: Differentially expressed genes (DEGs) between melanoma tissues and normal tissues were screened from the GSE 3,189 gene expression profile of Gene Expression Omnibus (GEO). A co-expression network was constructed by weighted correlation network analysis (WGCNA). Functional enrichment analysis for DEGs was performed. The risk prognostic model and nomogram predictive model were established utilizing the least absolute shrinkage and selection operator (LASSO) and Cox regression analysis.
Results: Using the differential expression analysis and WGCNA, 1,408 DEGs were screened between melanoma tissues and normal tissues. Functional enrichment analysis proved that these genes primarily participated in the cell cycle and mitotic phase regulation in cancer. In addition, 17 optimal DEGs were identified for constructing the risk score prognostic model. Cox regression analysis further revealed that ectonucleotide pyrophosphatase/phosphodiesterase 4 (ENPP4) and FGR proto-oncogene, Src family tyrosine kinase (FGR) were the key genes significantly associated with survival. A nomogram prediction model was established for individual survival probability by integrating pathological T/N/M stage, age, ENPP4, and FGR. High FGR or ENPP4 expression indicated a better prognosis in melanoma patients.
Conclusion: This study identified FGR and ENPP4 as potentially useful prognostic biomarkers for melanoma. The corresponding risk score prognostic model and nomogram may be a reliable tool for predicting the prognosis of melanoma patients.

Keywords: Ectonucleotide pyrophosphatase/phosphodiesterase 4 (ENPP4), FGR proto-oncogene, Melanoma, Nomogram, Prognosis, Src family tyrosine kinase (FGR)

1. Background

Melanoma is an aggressive tumor caused by melanocytes, mostly in the skin, but also visible in the mucosa and internal organs, accounting for about 3% of all tumors (1). patients with early melanoma may experience rapid enlargement of the original mole, swelling, shape or color change, and even itching, bleeding, as well as other symptoms and signs (2). The prognosis of early diagnosed non-metastatic primary cutaneous melanoma is generally satisfactory; nonetheless, metastatic melanoma is very fatal (3). The five-year survival rate of patients with metastatic melanoma is about 16% (4). Despite the utilization of surgery, chemotherapy, targeted therapy, and immunotherapy, the survival rate is still very low (4). The main risk factors for melanoma include sunburn, ultraviolet radiation, and anomalous moles; however, the specific molecular mechanism is still unclear (5). Therefore, the identification of new biomarkers for prognosis and early diagnosis is crucial in improving the survival rate of melanoma patients.

With the development of genomic microarray and high-throughput sequencing technology, bioinformatics analysis is rapidly becoming the mainstream method of cancer research. It has made great contributions to the identification of cancer-related biomarkers, the discovery of cancer mRNA vaccines, the prediction of prognosis, and the development of targeted therapies (6-10). On the basis of RNA sequencing, accumulating studies have identified differentially expressed genes (DEGs) as biomarkers involved in the development of different cancers (11-13), including melanoma. It has been verified that cyclooxygenase-2 (COX-2), which is an independent prognostic biomarker for melanoma, exerts a crucial function in melanoma development and chemoresistance (14). Centromere protein F (CENPF) plays a major role in the metastasis of melanoma and can be used as a prognostic biomarker (15).

PPARgamma coactivator 1 alpha (PGC1A) is a metabolic transcriptional coactivator that inhibits the metastasis of melanoma via suppressing oxidative stress injury (16). Sialidase neuraminidase 1 (NEU1) may act as a biomarker for melanoma cell growth and migration (17). Nevertheless, the application of relevant research in clinical practice is still very limited. Therefore, further research is still necessary to identify novel specific biomarkers to improve the prognosis of melanoma patients. Gene Expression Omnibus (GEO) belongs to an international public repository of microarrays, next-generation

sequencing, and other high-throughput forms of functional genomic data (18). It offers an opportunity for data mining of cancer gene expression profiles, which lays the foundation for promoting the early diagnosis, therapy, and prevention of various cancers (19).

In this study, a comprehensive analysis of microarray data from the GEO was used to identify differentially expressed genes in melanoma and normal tissues. Weighted gene co-expression network analysis (WGCNA) was applied to identify the key genes closely associated with melanoma progression. The biological function and signaling pathways associated with melanoma were assessed by functional enrichment analysis of DEGs. Furthermore, Cox regression analysis, least absolute shrinkage, and selection operator (LASSO) regression analysis were performed using clinical information and key genes to establish a risk prognosis model.

2. Objectives

The study aimed to identify the specific genes related to the prognosis of melanoma utilizing bioinformatics analyses.

3. Methods

DEGs Screening

We downloaded the GSE3189 dataset from the GEO database (https://www.ncbi.nlm.nih.gov/geo/). The GSE3189 dataset included 45 melanoma tissue samples and 18 normal nevi tissue samples (20). These data were normalized using the normalize Between Arrays function in the "limma" R package (21). The principal component analysis (PCA) was implemented by the "factoextra" R package. Thereafter, the limma package was employed for identifying the DEGs between the reference (ref) group and test group. DEGs were screened in accordance with the criterion ($P < 0.05$ and log $|FC| > 1$). In addition, ggplot2 was applied to make the volcano map and heat map to illustrate the differential expression of DEGs.

WGCNA

WGCNA (https://horvath.genetics.ucla.edu/html/CoexpressionNetwork/Rpackages/WGCNA/) on the GSE117613 dataset was performed by utilizing the WGCNA R package (22). The samples were subjected to the hierarchical clustering analysis for detecting and removing outliers. In accordance with the WGCNA user guides, the pickSoftThreshold function was employed to determine the best soft-threshold power to meet the scale-free topology criterion. We set the soft threshold of 7 to make the co-expression network meet the scale-free distribution. The adjacency matrix was transformed into a topological overlap matrix. Meanwhile, the WGCNA package was applied for clustering the matrix. The dynamic tree-cutting algorithm merged genes with similar expression patterns into the same module (module size = 30). Gene significance and module members were counted to assess the correlation between modules and melanoma. The module with the highest correlation with melanoma was selected. Venn analysis was carried out to screen out the common genes in the key module and DEGs.

Functional Enrichment Analysis

Gene Ontology (GO) enrichment analysis (https://www.geneontology.org/), Kyoto Encyclopedia of Genes, Genomes (KEGG) enrichment analysis (https://www.genome.jp/kegg/), and Gene Set Enrichment Analysis (GSEA) (https://www.gsea-msigdb.org/gsea/index.jsp) of DEGs were implemented utilizing the ClusterProfiler and Enrichplot packages of R (23, 24). The molecular Signatures Database (MsigDB) database (https://www.gsea-msigdb.org/gsea/msigdb) was used as a reference for GSEA. $|NES| \geq 1$ and $P < 0.05$ was considered statistically significant. The terms were visualized by utilizing the ggplot2 package.

Establishment of the Prediction Risk Model

Cox regression screening was carried out for prognostic DEGs with the R survival package (25). The LASSO regression analysis was implemented by the glmnet package to establish a predictive risk model (26), and 10-fold cross-validation for model construction was conducted. Risk score = Coefficient × gene expression. Patients were divided into the high-risk and low-risk groups, with the median risk score as the cut-off criterion. Kaplan-Meier analysis (https://kmplot.com/analysis/) and log-rank test were utilized to evaluate the difference in overall survival by R survival package.

Establishment of the Nomogram Prognosis Prediction Model

We established a prognostic nomogram combing gene expression with clinical information to predict 1-year survival in individual patients using the rms R package. Clinical parameters included age, pathologic T stage, pathologic N stage, and pathologic M stage. Decision curve analysis (DCA) was applied to determine the predictive model accuracy and the clinical utility of each model (27).

4. Results

Identification of DEGs in melanoma

We performed the difference analysis on the GSE3189 dataset. we observed the differences in gene expression between the ref group and the test group using PCA (Figure 1A). Using the limma package, we obtained DEGs of GSE3189, including 1157 downregulated genes and 975 upregulated

genes. The outcomes of the DEG analysis were represented as a volcano diagram and heatmap (Figure. 1B-C). The boxplots demonstrated that the expression distribution of samples was consistent, suggesting a good normalization (Figure 1D). All of these results illustrated that in GSE3189, there were 1,157 down-regulated genes and 975 up-regulated genes in melanoma.

Weighted gene co-expression network construction

To detect the key module most relevant to melanoma, WGCNA was performed on the GSE3189 dataset. The WGCNA package was written in R language. In order to establish a scale-free network, $\beta = 7$ (scale-free $R^2 = 0.86$) was selected as the optimum soft threshold value (Figure 2A-B). Modules of eigengenes were identified, and modules were clustered in accordance with their correlation. A total of 22 modules (dark olive green, royal blue, steel blue, blue, light cyan, pale turquoise, grey, dark red, light green, salmon, dark orange, black, cyan, violet, dark grey, dark magenta, dark turquoise, midnight blue, green, purple, grey 60, and magenta module) were identified in accordance with their co-expression pattern (Figure 2C-D). We discovered that the blue module was mostly associated with melanoma (Figure 2E). 1408 genes for melanoma were screened after taking the intersection of WGCNA (the blue module) and Limma (DEGs) (Figure 2F). All these results pointed out that after taking the intersection of WGCNA and Limma, a total of 1408 melanoma-related genes were screened.

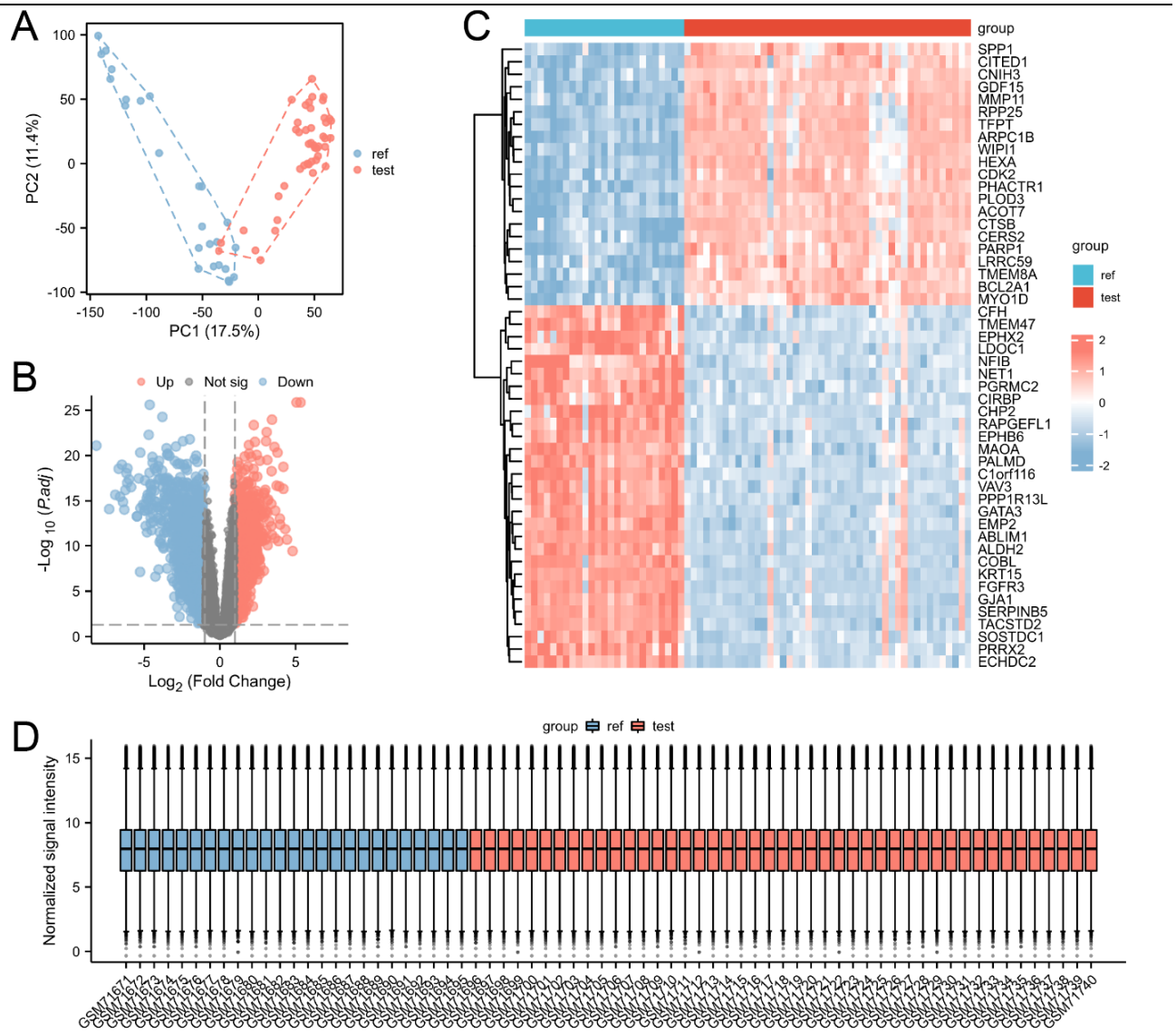

Figure 1. Identification of DEGs in melanoma
(A) PCA of the GSE3189 dataset visualizes the grouping information of samples. (B) The volcano diagram of all DEGs of the GSE3189 dataset. (C) Heatmap of the top 50 DEGs. (D) Boxplots of sample expression.

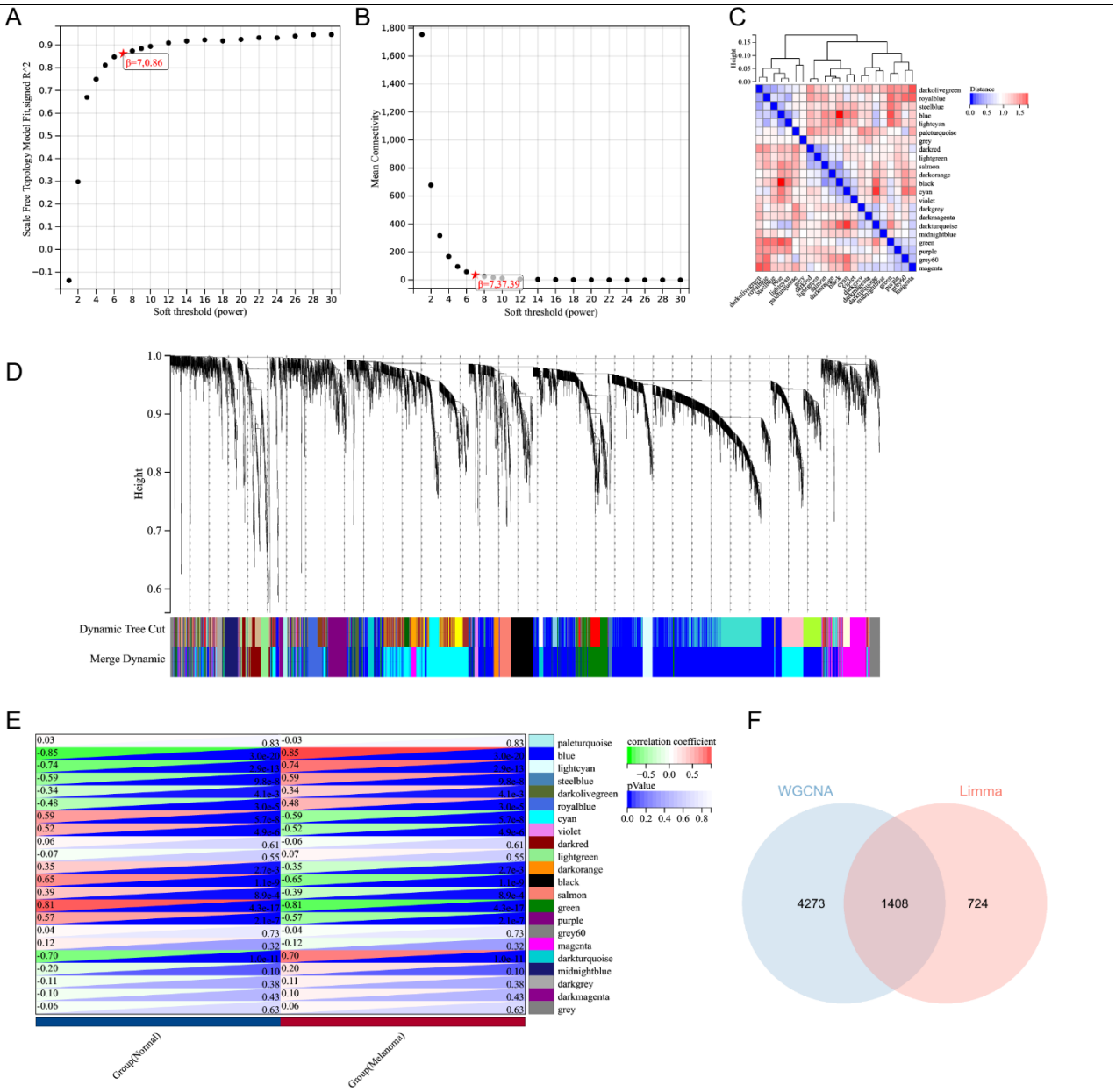

Figure 2. Weighted gene co-expression network establishment
(A-B) Scale-free fit index and mean connectivity are analyzed with assorted soft-threshold powers. (C) Hierarchical clustering of 22 module eigengenes. (D) Gene cluster dendrogram on the basis of module eigengenes. (E) The analysis of correlation of module eigengenes and normal group and melanoma group in a heatmap. (F) The Venn diagram shows the intersection of WGCNA and Limma.

GO and KEGG enrichment analysis of DEGs

GO and KEGG enrichment analyses were implemented to determine the biological functions of DEGs. GO analysis consisted of biological processes (BP), cellular components (CC), and molecular function (MF). As illustrated in Figure 3A-C, BP most commonly associated with DEGs were actin filament organization, regulation of actin cytoskeleton organization, and skin development. CC most commonly associated with DEGs were cell-cell junction, collagen-containing extracellular matrix, and cornified envelope. MF most commonly associated with DEGs were cadherin binding, structural constituent of cytoskeleton, and cell adhesion mediator activity. The significantly enriched KEGG terms were Axon guidance, Pathogenic Escherichia coli infection, and lysosome. Moreover, we further determined the enrichment of DEGs with Log2 FC in these biological functions. As displayed in Figure 3D-F, the relatively large amounts of DEGs were enriched in the collagen-containing extracellular matrix, cell-cell junction, actin filament organization, cornified envelope, regulation of actin cytoskeleton organization, and skin development. In addition, the enrichment of DEGs was most significant in lysosomes. All these results indicated that DEGs were enriched in the collagen-containing extracellular matrix, cell-cell junction, actin filament organization, cornified envelope, regulation of actin cytoskeleton organization, and skin development.

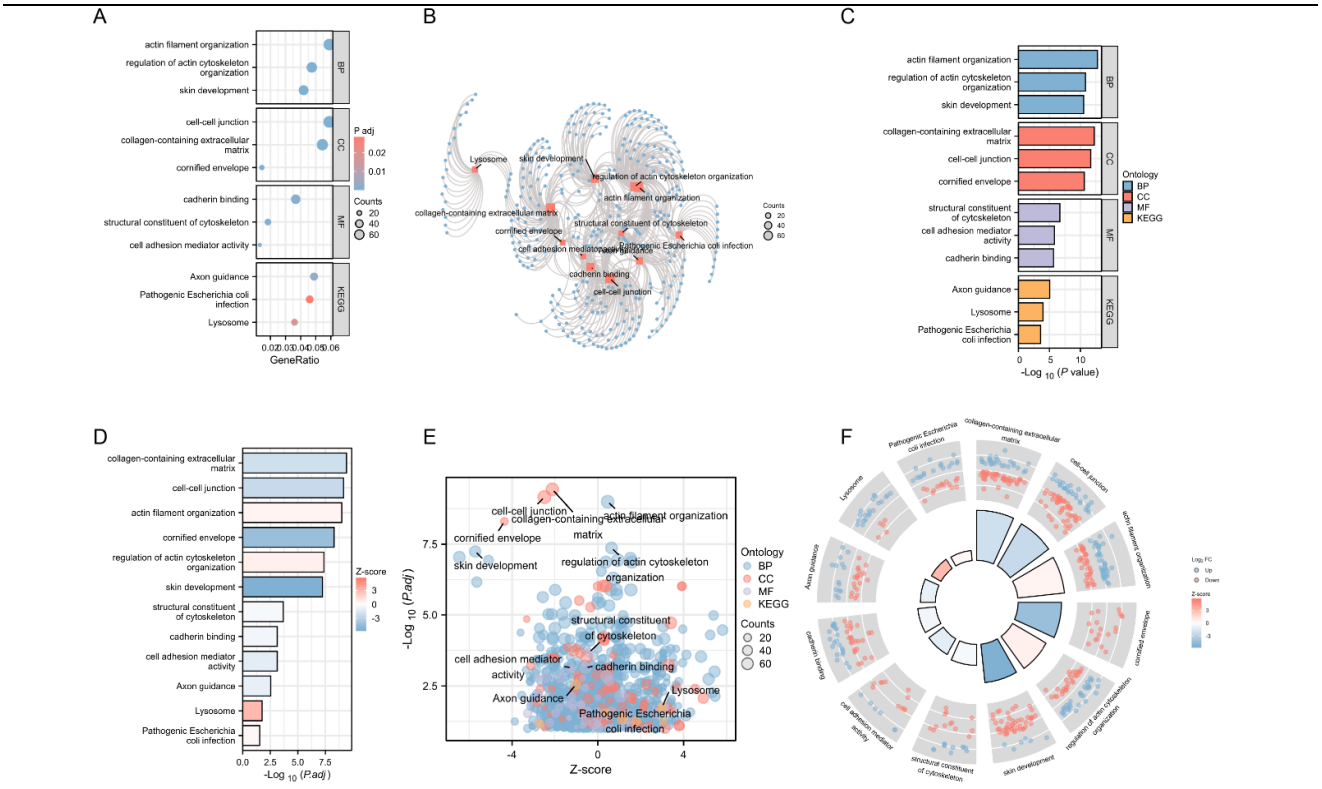

Figure 3. GO and KEGG enrichment analysis
(A)Bubble plot of the GO and KEGG enrichment analysis. (B) Gene network diagram of GO and KEGG pathways. (C-D) Bar graph of GO and KEGG enrichment results. Longer bars indicated more enriched DEGs. The red-to-blue color of Z-score signified a strong to weak enrichment. (E) Bubble plot of the GO and KEGG enrichment analysis. The size of the bubble represented the quantity of the DEGs. (F) The circle plot of GO and KEGG illustrated the scatter map of the LogFC of DEGs.

Function analysis of DEGs by GSEA

To investigate the function of DEGs further, we performed the GSEA utilizing the Reactome pathway database. As presented in Figure 4A-F, we found that DEGs were highly expressed in Mitotic prometaphase, RHO GTPases Activate Formins, Mitotic Metaphase and Anaphase, Mitotic Spindle Checkpoint, Separation of Sister Chromatids, Cell Cycle Mitotic, and Cell Cycle pathways. DEGs were lowly expressed in NABA Matrisome, Keratinization, Developmental Biology, and Formation of the Cornified Envelope pathways. All these results suggested that DEGs were involved in cell cycle and mitotic phase regulation.

Establishment and evaluation of predictive models

To establish an efficient model to predict prognosis, LASSO Cox regression analysis was performed on DEGs, and the candidate genes with the most powerful predictive features were identified (Fig. 5B-C). These genes were selected for constructing a risk score prognostic model. In accordance with the median risk score, melanoma patients were assigned to high or low-risk groups. The risk score plot and survival state scatter plot displayed that the high-risk group possessed lower survival and higher risk scores (Figure 5A). Furthermore, the heat map showed the expression file of 17 DEGs (DBNDD1, ICA1, KLHL13, M6PR, SNX11, LASP1, MAD1L1, WNT16, CD99, CYP51A1, SEMA3F, ENPP4, NIPAL3, NFYA, FGR, C1orf112, and TNMD) in risk groups (Figure 5A). Following that, univariate and multivariate Cox regression analysis was implemented, and ENPP4 and FGR were identified as key genes significantly associated with survival. We then established a nomogram for survival prediction of patients by integrating ENPP4, FGR, and clinical characteristics and scoring each feature. According to the actual situation of each sample, the total points were obtained by adding the scores corresponding to each factor.

The corresponding scale corresponded to the total score, thereby obtaining the 1-year survival probability of patients (Figure 5D). Kaplan-Meier survival curves displayed that high ENPP4 or FGR predicted a longer survival probability, while low ENPP4 or FGR predicted a shorter survival probability (Figure 5E-F). DCA was further performed to measure the net benefits of our model and we discovered that compared with a single factor, the positive results of all factors demonstrated the optimum clinical efficiency (Figure 5G-I). All these results suggested that ENPP4 and FGR functioned as crucial genes in predicting the prognosis of melanoma patients.

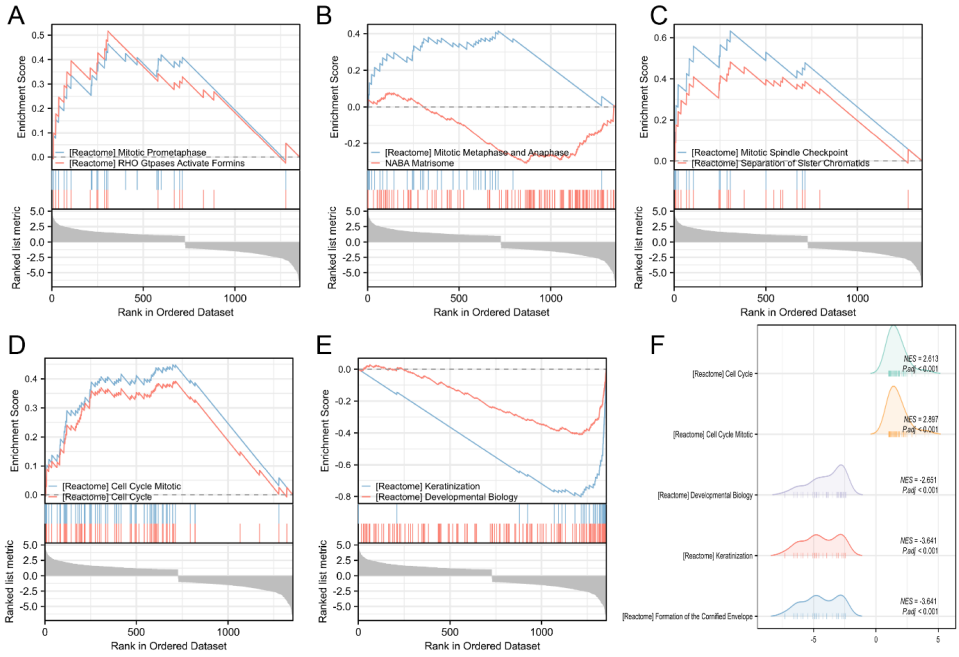

Figure 4. GSEA of DEGs utilizing the Reactome pathway database
(A-E) Typical GSEA enrichment plots for DEGs. (F) GSEA enrichment results exhibited in a ridge map.

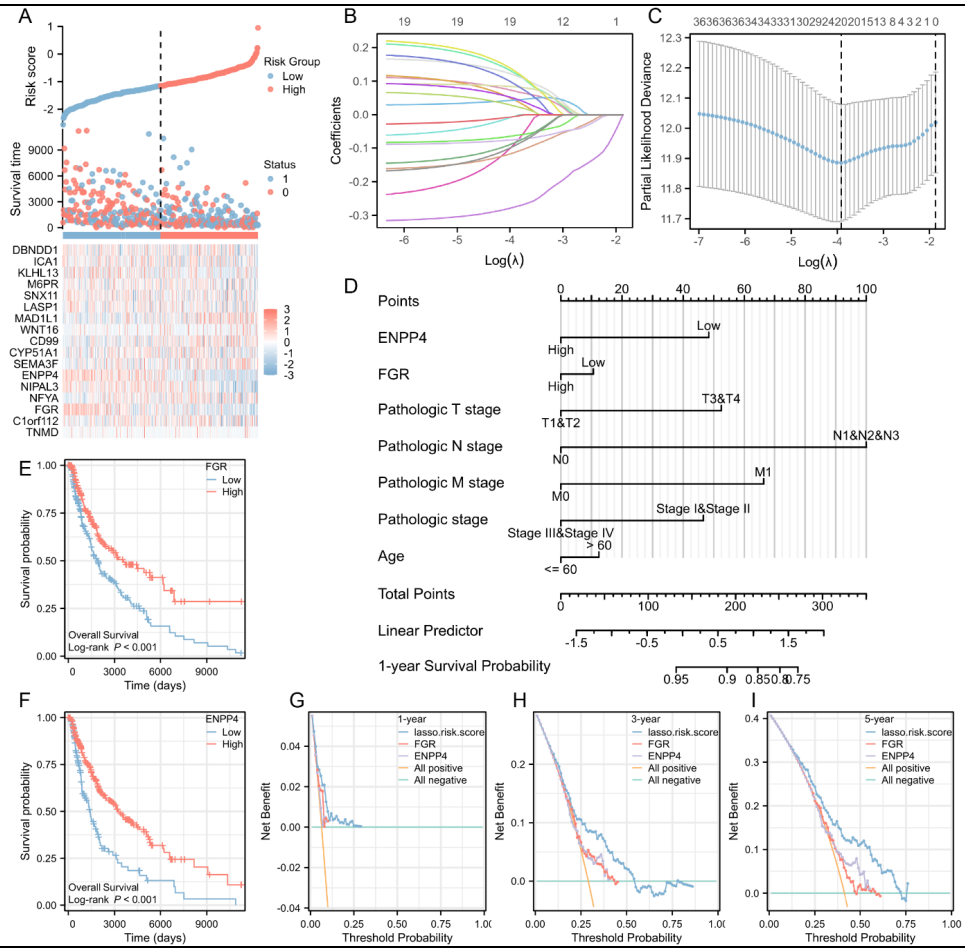

Figure 5. Establishment and evaluation of predictive models
(A) Survival probability of melanoma patients with high and low risk scores. (B) The distribution graph of LASSO regression analysis for DEGs. (C) Determination of penalty value by LASSO regression analysis. (D) A nomogram for the prognostic risk model. (E-F) Kaplan-Meier survival curves of melanoma patients with high and low expression of FGR or ENPP4. (G-I) DCA plots showed the net benefit generated by the prediction model.

Discussion

Melanoma is a common malignant skin tumor with a high metastatic rate, leading to a high mortality rate (28). Despite numerous studies on the molecular mechanisms of melanin in recent years (29), early diagnosis has not been achieved and patient prognosis has not improved. Therefore, it is necessary to understand the molecular mechanism involved in melanoma progression in depth. With the development of bioinformatics, more and more attention has been paid to the identification of biomarkers that can accurately predict prognosis (30). For instance, Zhang et al. suggested that GNGT1 and NMU can function as the combined diagnosis biomarkers of non-small-cell lung cancer (31). Zhou et al. revealed an eight-gene signature to predict the overall survival of colon cancer patients (32). Lin et al. indicated that NUDT1 may be an effective prognostic biomarker in clear cell renal cell carcinoma (33). The current study aimed to uncover novel predictive biomarkers and therapeutic targets for melanoma by bioinformatics analysis.

Herein, we performed a differential analysis of the GSE3189 dataset and identified 2132 DEGs between melanoma tissues and control tissues, including 1157 downregulated genes and 975 upregulated genes. WGCNA provided module construction and correlation analysis to affirm the association between genes and melanoma. We found that DEGs were divided into 22 gene co-expression modules and proved that the blue module was significantly associated with melanoma patients. After taking the intersection of Limma and WGCNA, we obtained 1408 genes. Furthermore, GO and KEGG analysis demonstrated that genes were enriched in actin filament organization, regulation of actin cytoskeleton organization, skin development, cell-cell junction, collagen-containing extracellular matrix, cornified envelope, cadherin binding, structural constituent of cytoskeleton, cell adhesion mediator activity, and pathway of axon guidance, pathogenic escherichia coli infection, and lysosome.

The GSEA enrichment analysis further proved that genes were associated with cell cycle and mitotic phase regulation. These findings suggested that these genes were closely related to melanoma development. Moreover, LASSO regression analysis determined 17 genes as the risk factors for melanoma patients. The COX regression analysis and a nomogram for survival prediction further proved that ENPP4 and FGR genes were the optimum prognostic genes. We proved that ENPP4 and FGR were notably correlated with the survival of melanoma patients. Overexpressed ENPP4 and FGR were the protective factors related to good prognosis.

ENPP4 is a procoagulant enzyme on the surface of vascular endothelium, belonging to the ectonucleotide pyrophosphatase/phosphodiesterase family (34). The dysregulation of this family has been confirmed to take part in inflammation, cell migration, invasion, and angiogenesis (35). Currently, there is limited evidence on the biological function of ENPP4 in malignant tumors. Nonetheless, the ENPP family has been reported to promote the tumorigenesis and metastasis of breast cancer and glioblastoma (34, 36). Studies have confirmed that ENPP4 can inhibit cell proliferation through direct or indirect contact with ATP or insulin receptors on the surface of tumor cells (37).

ENPP4 has been reported to catalyze the extracellular ATP released from tumor cells and decrease the combination of ATP and its receptor (37). Furthermore, ENPP4 can contact the insulin receptor and suppress its activity (38). In addition, ENPP4 might be a biomarker for the prognosis of patients with Barrett's esophagus (39). More importantly, a bioinformatics analysis proposed by Yao et al. pointed out that ENPP4 is downregulated in lung squamous cell carcinoma and may be a prognostic biomarker for lung squamous cell carcinomas (40). In line with the stated study, the present research suggested that ENPP4 may be a potential prognostic biomarker for melanoma related to good prognosis. However, the specific role of ENPP4 in melanoma needs further investigation.

Tyrosine kinase FGR is one of the members of Src family kinases (SFKs) family (41). SFKs are a group of enzymes that play a key role in cell proliferation, adhesion, and differentiation of human cancers (42). Studies have confirmed that FGR is involved in macrophage activation, insulin resistance, and liver steatosis (43). FGR upregulation has been discovered to be correlated with aggressive tumor characteristics and lower survival time in patients with leukemia (44), lymphoma (45), or glioma (46). Studies have revealed that FGR is expressed at a high level in human acute myeloid leukemia samples, and its depletion can suppress cell growth (47, 48). A small-molecule inhibitor of FGR has been reported to block the radiation fibrosis pathway (49). Inconsistent with the aforementioned studies, the current research found that high FGR expression predicted a good survival of melanoma patients, which may be related to tumor heterogeneity. Nevertheless, the biological role of FGR in melanoma needs to be further explored.

There are some limitations in this study. Firstly, we utilized retrospective data from public databases to construct and verify our prognostic model. Secondly, we did not perform functional experiments on ENPP4 and FGR in vivo or in vitro. Therefore, the specific mechanism of ENPP4 and FGR in melanoma progression has not been demonstrated. In the future, combining ENPP4 and FGR with clinical indicators to establish an ideal prediction model will be conducive to the early prediction of metastasis and metastasis-free survival. In addition, we will also

use ENPP4 and FGR in our future research to investigate whether they can be used as therapeutic targets.

6. Conclusion

In this study, the key genes ENPP4 and FGR involved in the development of melanoma were identified by bioinformatics methods, and a prognostic risk model was effectively constructed to indicate that ENPP4 and FGR could be used as prognostic biomarkers for melanoma. The present study may provide new insights into the treatment of melanoma.

Acknowledgments

None

Footnotes

Conflicts of Interest: There is nothing to declare.

Author Contribution: Conceptualization and methodology, Xuelian Zou; Data collection, Tingting Li; Data analysis and interpretation, Xiangyue Zhang; Drafting the article, Xiaojing Kang; Revising and final approval of the manuscript, all authors.

Funding: This study received funding from the Key R&D tasks of the Xinjiang Autonomous Region in 2021 (2021B03001).

Ethical Statements: Not applicable.

References

1. Rastrelli M, Tropea S, Rossi CR, Alaibac M. Melanoma: epidemiology, risk factors, pathogenesis, diagnosis and classification. *In Vivo*. 2014;**28**(6):1005-11. [PubMed: 25398793].
2. Darmawan CC, Jo G, Montenegro SE, Kwak Y, Cheol L, Cho KH, et al. Early detection of acral melanoma: A review of clinical, dermoscopic, histopathologic, and molecular characteristics. *J Am Acad Dermatol*. 2019;**81**(3):805-12. doi: 10.1016/j.jaad.2019.01.081. [PubMed: 30731177].
3. Kudchadkar RR, Lowe MC, Khan MK, McBrien SM. Metastatic melanoma. *CA Cancer J Clin*. 2020 ;**70**(2):78-85. doi: 10.3322/caac.21599. [PubMed: 32101327].
4. Davis LE, Shalin SC, Tackett AJ. Current state of melanoma diagnosis and treatment. *Cancer Biol Ther*. 2019;**20**(11):1366-79. doi: 10.1080/15384047.2019.1640032. [PubMed: 31366280].
5. Chattopadhyay C, Kim DW, Gombos DS, Oba J, Qin Y, Williams MD, et al. Uveal melanoma: From diagnosis to treatment and the science in between. Cancer. 2016;**122**(15):2299-312. doi: 10.1002/cncr.29727. [PubMed: 26991400].
6. Pareek CS, Smoczynski R, Tretyn A. Sequencing technologies and genome sequencing. *J Appl Genet*. 2011;**52**(4):413-35. doi: 10.1007/s13353-011-0057-x. [PubMed: 21698376].
7. Ji F, Sadreyev RI. RNA-seq: Basic Bioinformatics Analysis. *Curr Protoc Mol Biol*. 2018;**124**(1):e68. doi: 10.1002/cpmb.68. [PubMed: 30222249].
8. Tao Z, Shi A, Li R, Wang Y, Wang X, Zhao J. Microarray bioinformatics in cancer- a review. *J BUON*. 2017;**22**(4):838-43. [PubMed: 29155508].
9. Zeng X, Shi G, He Q, Zhu P. Screening and predicted value of potential biomarkers for breast cancer using bioinformatics analysis. *Sci Rep*. 2021;**11**(1):20799. doi: 10.1038/s41598-021-00268-9. [PubMed: 34675265].
10. Hammad A, Elshaer M, Tang X. Identification of potential biomarkers with colorectal cancer based on bioinformatics analysis and machine learning. *Math Biosci Eng*. 2021;**18**(6):8997-9015. doi: 10.3934/mbe.2021443. [PubMed: 34814332].
11. Mao Y, Shen J, Lu Y, Lin K, Wang H, Li Y, et al. RNA sequencing analyses reveal novel differentially expressed genes and pathways in pancreatic cancer. *Oncotarget*. 2017;**8**(26):42537-47. doi: 10.18632/oncotarget.16451. [PubMed: 28418924].
12. Kim N, Gim JA, Lee BJ, Choi BI, Park SB, Yoon HS, et al. RNA-sequencing identification and validation of genes differentially expressed in high-risk adenoma, advanced colorectal cancer, and normal controls. *Funct Integr Genomics*. 2021;**21**(3-4):513-21. doi: 10.1007/s10142-021-00795-8. [PubMed: 34273035].
13. Lei T, Qian H, Lei P, Hu Y. Ferroptosis-related gene signature associates with immunity and predicts prognosis accurately in patients with osteosarcoma. *Cancer Sci*. 2021;**112**(11):4785-98. doi: 10.1111/cas.15131. [PubMed: 34506683].
14. Tudor DV, Bâldea I, Lupu M, Kacso T, Kutasi E, Hopârtean A, et al. COX-2 as a potential biomarker and therapeutic target in melanoma. *Cancer Biol Med*. 2020;**17**(1):20-31. doi: 10.20892/j.issn.2095-3941.2019.0339. [PubMed: 32296574].
15. Li M, Zhao J, Yang R, Cai R, Liu X, Xie J, et al. CENPF as an independent prognostic and metastasis biomarker corresponding to CD4+ memory T cells in cutaneous melanoma. *Cancer Sci*. 2022 ;**113**(4):1220-34. doi: 10.1111/cas.15303. [PubMed: 35189004].
16. Luo C, Lim JH, Lee Y, Granter SR, Thomas A, Vazquez F, et al. A PGC1α-mediated transcriptional axis suppresses melanoma metastasis. *Nature*. 2016;**537**(7620):422-26. doi: 10.1038/nature19347. [PubMed: 27580028].
17. Peng Q, Gao L, Cheng HB, Wang JS, Wang J. Sialidase NEU1 May Serve as a Potential Biomarker of Proliferation, Migration and Prognosis in Melanoma. *World J Oncol*. 2022;**13**(4):222-34. doi: 10.14740/wjon1509. [PubMed: 36128592].
18. Clough E, Barrett T. The Gene Expression Omnibus Database. *Methods Mol Biol*. 2016;**1418**:93-110. doi: 10.1007/978-1-4939-3578-9_5. [PubMed: 27008011].
19. Zhao J, Guo C, Ma Z, Liu H, Yang C, Li S. Identification of a novel gene expression signature associated with overall survival in patients with lung adenocarcinoma: A comprehensive analysis based on TCGA and GEO databases. *Lung Cancer*. 2020;**149**:90-96. doi: 10.1016/j.lungcan.2020.09.014. [PubMed: 33002836].
20. Talantov D, Mazumder A, Yu JX, Briggs T, Jiang Y, Backus J, et al. Novel genes associated with malignant melanoma but not benign melanocytic lesions. *Clin Cancer Res*. 2005;**11**(20):7234-42. doi: 10.1158/1078-0432.CCR-05-0683. [PubMed: 16243793].
21. Ritchie ME, Phipson B, Wu D, Hu Y, Law CW, Shi W, et al. limma powers differential expression analyses for RNA-sequencing and microarray studies. *Nucleic Acids Res*. 2015;**43**(7):e47. doi: 10.1093/nar/gkv007. [PubMed: 25605792].
22. Tian Z, He W, Tang J, Liao X, Yang Q, Wu Y, et al. Identification of Important Modules and Biomarkers in Breast Cancer Based on WGCNA. *Onco Targets Ther*. 2020;**13**:6805-17. doi: 10.2147/OTT.S258439. [PubMed: 32764968].
23. Wu T, Hu E, Xu S, Chen M, Guo P, Dai Z, et al. clusterProfiler 4.0: A universal enrichment tool for interpreting omics data. *Innovation (Camb)*. 2021;**2**(3):100141. doi: 10.1016/j.xinn.2021.100141. [PubMed: 34557778].
24. Liu XS, Zhou LM, Yuan LL, Gao Y, Kui XY, Liu XY, et al. NPM1 Is a Prognostic Biomarker Involved in Immune Infiltration of Lung Adenocarcinoma and Associated With m6A Modification and Glycolysis. *Front Immunol*. 2021;**12**:724741. doi: 10.3389/fimmu.2021.724741. [PubMed: 34335635].
25. Barros AJ, Hirakata VN. Alternatives for logistic regression in cross-sectional studies: an empirical comparison of models that directly estimate the prevalence ratio. *BMC Med Res Methodol*. 2003;**3**:21. doi: 10.1186/1471-2288-3-21. [PubMed: 14567763].
26. Tang G, Qi L, Sun Z, Liu J, Lv Z, Chen L, et al. Evaluation and analysis of incidence and risk factors of lower extremity venous thrombosis after urologic surgeries: A prospective two-center cohort study using LASSO-logistic regression. *Int J Surg*. 2021;**89**:105948. doi: 10.1016/j.ijsu.2021.105948. [PubMed: 33892158].

27. Vickers AJ, Holland F. Decision curve analysis to evaluate the clinical benefit of prediction models. *Spine J*. 2021;**21**(10):1643-48. doi: 10.1016/j.spinee.2021.02.024. [PubMed: 33676020].
28. Bobos M. Histopathologic classification and prognostic factors of melanoma: a 2021 update. *Ital J Dermatol Venerol*. 2021;**156**(3):300-21. doi: 10.23736/S2784-8671.21.06958-3. [PubMed: 33982546].
29. Huang AC, Zappasodi R. A decade of checkpoint blockade immunotherapy in melanoma: understanding the molecular basis for immune sensitivity and resistance. *Nat Immunol*. 2022;**23**(5):660-70. doi: 10.1038/s41590-022-01141-1. [PubMed: 35241833].
30. Xu Y, Zhang P, Zhang K, Huang C. The application of CA72-4 in the diagnosis, prognosis, and treatment of gastric cancer. *Biochim Biophys Acta Rev Cancer*. 2021;**1876**(2):188634. doi: 10.1016/j.bbcan.2021.188634. [PubMed: 34656687].
31. Zhang JJ, Hong J, Ma YS, Shi Y, Zhang DD, Yang XL, et al. Identified GNGT1 and NMU as Combined Diagnosis Biomarker of Non-Small-Cell Lung Cancer Utilizing Bioinformatics and Logistic Regression. *Dis Markers*. 2021;**2021**:6696198. doi: 10.1155/2021/6696198. [PubMed: 33505535].
32. Zhou L, Yu Y, Wen R, Zheng K, Jiang S, Zhu X, et al. Development and Validation of an 8-Gene Signature to Improve Survival Prediction of Colorectal Cancer. *Front Oncol*. 2022;**12**:863094. doi: 10.3389/fonc.2022.863094. [PubMed: 35619909].
33. Lin Y, Zhang F, Jin Y, Zhong Q, Tan W, Liu J, et al. NUDT1 Could Be a Prognostic Biomarker and Correlated with Immune Infiltration in Clear Cell Renal Cell Carcinoma. *Appl Bionics Biomech*. 2022;**2022**:3669296. doi: 10.1155/2022/3669296. [PubMed: 36606241].
34. Albright RA, Chang WC, Robert D, Ornstein DL, Cao W, Liu L, et al. NPP4 is a procoagulant enzyme on the surface of vascular endothelium. *Blood*. 2012;**120**(22):4432-40. doi: 10.1182/blood-2012-04-425215. [PubMed: 22995898].
35. Albright RA, Ornstein DL, Cao W, Chang WC, Robert D, Tehan M, et al. Molecular basis of purinergic signal metabolism by ectonucleotide pyrophosphatase/phosphodiesterases 4 and 1 and implications in stroke. *J Biol Chem*. 2014;**289**(6):3294-306. doi: 10.1074/jbc.M113.505867. PubMed: 24338010].
36. Kishi Y, Okudaira S, Tanaka M, Hama K, Shida D, Kitayama J, et al. Autotaxin is overexpressed in glioblastoma multiforme and contributes to cell motility of glioblastoma by converting lysophosphatidylcholine to lysophosphatidic acid. *J Biol Chem*. 2006;**281**(25):17492-500. doi: 10.1074/jbc.M601803200. [PubMed: 16627485].
37. Chin CN, Dallas-Yang Q, Liu F, Ho T, Ellsworth K, Fischer P, et al. Evidence that inhibition of insulin receptor signaling activity by PC-1/ENPP1 is dependent on its enzyme activity. *Eur J Pharmacol*. 2009;**606**(1-3):17-24. doi: 10.1016/j.ejphar.2009.01.016. [PubMed: 19374858].
38. Salisbury TB, Tomblin JK. Insulin/Insulin-like growth factors in cancer: new roles for the aryl hydrocarbon receptor, tumor resistance mechanisms, and new blocking strategies. *Front Endocrinol (Lausanne)*. 2015;**6**:12. doi: 10.3389/fendo.2015.00012. [PubMed: 25699021].
39. Wang J, Di J, Wang G. ENPP4 overexpression is associated with no recovery from Barrett's esophagus. *Int J Clin Exp Pathol*. 2020;**13**(12):2927-36. [PubMed: 33425094].
40. Yao Y, Zhang T, Qi L, Liu R, Liu G, Wang X, et al. Competitive Endogenous RNA Network Construction and Comparison of Lung Squamous Cell Carcinoma in Smokers and Nonsmokers. *Dis Markers*. 2019;**2019**:5292787. doi: 10.1155/2019/5292787. [PubMed: 31885738].
41. Gutkind JS, Robbins KC. Translocation of the FGR protein-tyrosine kinase as a consequence of neutrophil activation. *Proc Natl Acad Sci USA*. 1989;**86**(22):8783-7. doi: 10.1073/pnas.86.22.8783. [PubMed: 2682659].
42. Iriyama N, Yuan B, Hatta Y, Takagi N, Takei M. Lyn, a tyrosine kinase closely linked to the differentiation status of primary acute myeloid leukemia blasts, associates with negative regulation of all-trans retinoic acid (ATRA) and dihydroxyvitamin D3 (VD3)-induced HL-60 cells differentiation. *Cancer Cell Int*. 2016;**16**:37. doi: 10.1186/s12935-016-0314-5. [PubMed: 27182202].
43. Acín-Pérez R, Iborra S, Martí-Mateos Y, Cook ECL, Conde-Garrosa R, Petcherski A, et al. Fgr kinase is required for proinflammatory macrophage activation during diet-induced obesity. *Nat Metab*. 2020;**2**(9):974-88. doi: 10.1038/s42255-020-00273-8. [PubMed: 32943786].
44. Hu Y, Liu Y, Pelletier S, Buchdunger E, Warmuth M, Fabbro D, et al. Requirement of Src kinases Lyn, Hck and Fgr for BCR-ABL1-induced B-lymphoblastic leukemia but not chronic myeloid leukemia. *Nat Genet*. 2004;**36**(5):453-61. doi: 10.1038/ng1343. [PubMed: 15098032].
45. Sharp NA, Luscombe MJ, Clemens MJ. Regulation of c-fgr proto-oncogene expression in Burkitt's lymphoma cells: effect of interferon treatment and relationship to EBV status and c-myc mRNA levels. *Oncogene*. 1989;**4**(8):1043-6. [PubMed: 2548145].
46. Hui AB, Lo KW, Yin XL, Poon WS, Ng HK. Detection of multiple gene amplifications in glioblastoma multiforme using array-based comparative genomic hybridization. *Lab Invest*. 2001;**81**(5):717-23. doi: 10.1038/labinvest.3780280. [PubMed: 11351043].
47. Weir MC, Shu ST, Patel RK, Hellwig S, Chen L, Tan L, et al. Selective Inhibition of the Myeloid Src-Family Kinase Fgr Potently Suppresses AML Cell Growth in Vitro and in Vivo. *ACS Chem Biol*. 2018;**13**(6):1551-59. doi: 10.1021/acschembio.8b00154. [PubMed: 29763550].
48. Dos Santos C, McDonald T, Ho YW, Liu H, Lin A, Forman SJ, et al. The Src and c-Kit kinase inhibitor dasatinib enhances p53-mediated targeting of human acute myeloid leukemia stem cells by chemotherapeutic agents. *Blood*. 2013;**122**(11):1900-13. doi: 10.1182/blood-2012-11-466425. [PubMed: 23896410].
49. Mukherjee A, Epperly MW, Shields D, Hou W, Fisher R, Hamade D, et al. Ionizing irradiation-induced Fgr in senescent cells mediates fibrosis. *Cell Death Discov*. 2021;**7**(1):349. doi: 10.1038/s41420-021-00741-4. [PubMed: 34772919].